Available online at www.sciencedirect.com

ScienceDirect

Proceedings of the Combustion Institute 38 (2021) 5249–5257

Proceedings of the Combustion Institute

www.elsevier.com/locate/proci

Experimental and computational investigations of ethane and ethylene kinetics with copper oxide particles for Chemical Looping Combustion

Christopher M. Burger [a,*], Wenbo Zhu [b], Guoming Ma [a], Hao Zhao [a], Adri C.T. van Duin [b], Yiguang Ju [a]

[a] *Department of Mechanical and Aerospace Engineering, Princeton University, Princeton, NJ 08544-5263, USA*
[b] *Department of Mechanical Engineering, Pennsylvania State University, University Park, PA 16802, USA*

Received 8 November 2019; accepted 9 June 2020
Available online 23 January 2021

Abstract

In this work, reaction pathways for the oxidation of methane, ethane, and ethylene with CuO was obtained by ReaxFF Molecular Dynamics (MD) simulations between temperatures of 1000 K and 2000 K. Experiments in a fixed-bed flow reactor were preformed with methane, ethane, and ethylene at temperatures ranging from 500 K to 1000 K with time-dependent species measurements from an Electron-Ionization Molecular Beam Mass Spectrometer (MBMS), and species validation with Gas Chromatography (GC) for detection of complete and intermediate combustion products. The MBMS and GC allow for the detection of oxygenated species and larger species produced from radical reformation. The simulation and experiment agree on the production of such species as CH_3CHO, CH_2O, CO, and H_2O, which allow for the creation of simple C1 and C2 reaction pathways, which can be used in kinetic models of C2 species and larger fuels such as biofuels, which inherently depend on C1 and C2 kinetics and reaction pathway. The simulation and experiment disagree on the formation of C_2H_2, CH_3OH, and CO_2, with large amounts of C_2H_2 being measured in the ethylene oxidation simulations and CH_3OH being formed in methane oxidation simulations, while neither species were experimentally found. In the case of CO_2, large amounts of CO_2 are rapidly produced in experiments with C2 fuels at 800 K, while little-to-no CO_2 was observed in simulations. This is believed to be resulting from the extremely short timescale of the simulations, preventing total oxidation of the fuel. The differences in products produced between simulation and experiment allow for the potential to modify the ReaxFF potential functions to more accurately model the experimental products of Cu–H–O–C reaction kinetics.

Keywords: Chemical-Looping Combustion; Oxygen carrier; Copper oxide; ReaxFF; Fixed-bed flow reactor

* Corresponding author.
E-mail address: cburger@princeton.edu (C.M. Burger).
https://doi.org/10.1016/j.proci.2020.06.006

1. Introduction

Chemical Looping Combustion (CLC) is an emerging power generation method that has application to Carbon Capture and Sequestration (CCS) due to the high concentration of CO_2 that can be produced. This process involves a metal oxide as an oxygen carrier which transfers oxygen between an air supply and a fuel supply. Fuels proposed for such a process include coal, syngas, natural gas, and various biofuels [1]. While Light Hydrocarbons (LHCs), for example C2–C5, are often not directly proposed as a fuel supply, it is often found that mixed amounts of these species are present in common fuel supplies. For example, crude natural gas can potentially contain up to 10 vol% of LHCs [2]. LHCs can also be formed through radical recombination reactions from species like methane, or can be formed in reactions of much larger fuels such as biofuels. This area of LHC kinetics with CuO has not been thoroughly explored from investigations into CLC technology. Previous work has often been done studying the kinetics of light fuels such as H_2, CH_4, and CO, with the chemistry often described through one-step, or few-step chemistry. Monazam et al. [3] presented work on the reduction of CuO by methane, assuming one-step chemistry while ranging the concentration of methane from 20% to 100% CH_4 concentration. They found no de-activation of the particles throughout 10 oxidation and reduction cycles at any CH_4 concentration. Goldstein et al. [4] described the oxidation of CuO with CO with kinetics including 9 reactions steps, having included absorption and desorption reactions and reactions for different oxides of copper.

Compared to the lightest of fuels like H_2, CO and CH_4, which have been heavily covered in the literature, the C2–C5 hydrocarbons have a lack of experimental data to validate models and reaction schemes with. There currently lacks an understanding of the reaction mechanisms and kinetics for LHCs. Experimental data and corresponding reaction mechanisms for the LHCs are needed to better the models used for CLC.

The objective of this paper is to determine the important reaction steps involved with the oxidation of methane, ethane, and ethylene with CuO particles at different temperatures. To this end, experimental and computational work analyzing the product species resulting from such oxidation, was preformed. From the experimental and computational results, reaction mechanisms for the three fuels were created.

2. Experimental methods

2.1. Fixed-bed flow reactor and species detection

All experiments were performed in a laminar flow reactor modified in a fixed-bed configuration.

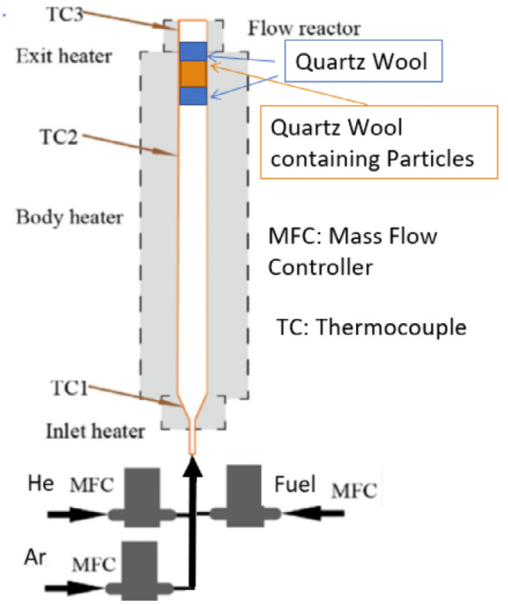

Fig. 1. Schematic of fixed bed flow reactor with CuO particles.

Figure 1 shows the schematic of the fixed-bed reactor. The fixed-bed is composed of a 17 mm inner diameter tube that is 320 mm in length. Reactants are supplied through mass flow controllers and enter the system at the bottom of the tube in a 100 mm long, 2 mm wide inner diameter inlet. The quartz tube is placed in a stainless steel jacket, which itself was placed in a 3-stage heating unit for temperature control. The maximum temperature deviation of ±4 K from the setting temperature has been measured throughout the length of the reactor. Towards the top of the quartz tube, the particle-containing quartz wool sample was placed between two pieces of quartz wool, to prevent the loss of particles during the experiment. An electron-ionization MBMS was used to make time-dependent measurements of C_2H_6, C_2H_4, C_2H_2, CO_2, and H_2O at the exit of the flow reactor. The details of the EI-MBMS operation and calibration techniques are described elsewhere [5]. In addition to the MBMS measurements, a μ-GC (Inficon 3000) is used to detect and measure stable species within a 5% uncertainty, the details of which are described elsewhere [6]. Measurements with the MBMS have an uncertainly of 20%, which results from the accuracy of the calibrations and the control over the electron energy in the MBMS (20 eV ± 1 eV). Time-dependent species measurements with the MBMS occurred roughly three times per second, while GC measurements required multiple minutes in-between each measurement.

2.2. Sample preparation

The copper oxide particles used in this investigation were <10 micron 98% copper oxide particles from Sigma Aldrich. The samples were prepared by dispersing the particles evenly throughout quartz wool. This was achieved by mixing and solution of 3 g of copper oxide particles and 0.5 g of quartz wool in deionized water, then placing the mixture in ultrasonic bath for 1 h to disperse particles through the wool. The particle-containing quartz wool was then place in an oven to dry for 8-h, with a resulting sample of 0.5 g of quartz wool containing roughly 2.00 g of copper oxide. The samples were weighed at each stage of the preparation to determine the error in preparation, and the particles added or removed from the prepared sample resulted in samples of 2.00 g ±0.05 g.

2.3. Experimental conditions

The experiments were performed at atmospheric pressure with the inlet volumetric flow rate fixed at 200 ml/min at 293 K. Fuel concentration was fixed at 5%, with 7.5% argon and 87.5% Helium composing the reminder of the species. Temperature was varied to 500 K and 800 K for ethane and ethylene, and 1000 K methane, with the maximum reactor temperature constrained by the thermal decomposition of the fuels.

3. Computational methods

3.1. Methodology

ReaxFF is an empirical force field method to investigate the properties of molecules and solids utilizing reactive bond order [7]. The quantum chemistry (QC) methods can accurately describe molecular systems, however are only practical for small systems because of its high computational intensity [8]. In large molecular systems, the generic force fields (FF) like DREIDING [9] and UFF [10] are commonly utilized, but they cannot describe chemical reactions because of their fixed bond parameters. To fill the gap between the QC and FF, Reactive Force Field (ReaxFF) was developed. Like other empirical nonreactive force field, the system energy in ReaxFF is divided into contributions from partial energies as shown in Eq. (1) [12].

$$E_{system} = E_{Bond} + E_{over} + E_{under} + E_{val} + E_{pen} + E_{tors} + E_{conj} + E_{vdWaals} + E_{Coloumb} \quad (1)$$

These partial energies are associated with the bond, over coordination, under coordination, valence angle, penalty, torsion, conjugation, van der Waals, and Coulomb interactions respectively. In force field potentials, these partial energy contributions are bond order dependent. To describe a reactive

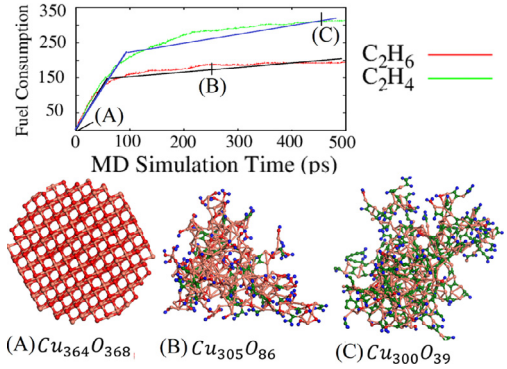

Fig. 2. Fuel consumption analysis for ethane and ethylene in our NVT MD simulation at 2000 K. It indicates that both fuels contain 2-stage kinetics influenced by surface reaction and oxygen diffusion.

system energy, ReaxFF applies the concept of the reactive bond order in which the bond order is dependent on the bond distance shown in Eq. (2).

$$BO'_{ij} = exp[p_{bo,1} * (r_{ij}/r_o)^{p_{bo,2}}] + exp\left[p_{bo,3} * \left(r^{\pi}_{ij}/r_o\right)^{p_{bo,4}}\right] + exp\left[p_{bo,5} * \left(r^{\pi,\pi}_{ij}/r_o\right)^{p_{bo,6}}\right] \quad (2)$$

This reactive bond order is dependent on sigma (pbo1/pbo2), pi (pbo3/pbo4), and double pi (pbo5/pbo6) bonds respectively. For a more detailed description of the ReaxFF method, please refer to a recent review paper by Senftle and co-workers [13]. Additional information on the development of the force field can be found in Supplementary materials.

3.2. Simulation detail

3.2.1. Simulating CuO/C2 species interactions using Cu/C/H/O ReaxFF

A series of 500 ps molecular dynamics (MD) simulations were preformed utilizing a Cu/C/H/O force field. A spherical 12 Å radius CuO nanoparticle was placed in the center of the 70 × 70 × 70 Å cubic cell surrounded by 400 ethane (C_2H_6) or ethylene (C_2H_4) molecules. Considering the time scale in the simulation, the low temperature simulation is not directly comparable with experiment results. An NVT ensemble with Berendsen thermostat with a damping constant of 0.1 ps was applied at 2000 K.

3.2.2. Simulating CuO/CH_3 radicals interactions using Cu/C/H/O ReaxFF

A series of 250 ps MD simulations were preformed utilizing the Cu/C/H/O force field. A spherical 12 Å radius CuO nanoparticle was placed in the center of the 70 × 70 × 70 Å cubic cell. From the previous simulations, the methane (CH_4) molecules were not reactive at low temperature (2000 K). CH_3

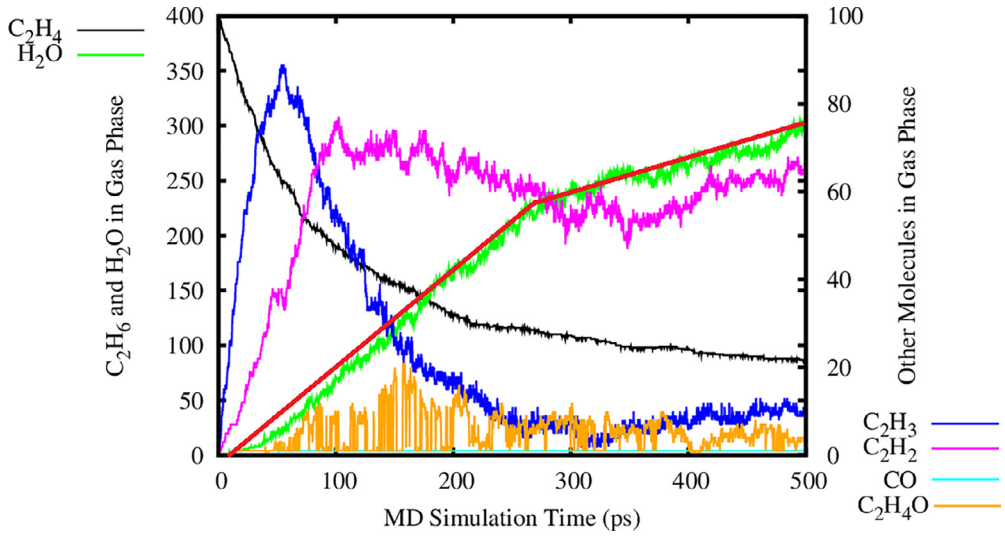

Fig. 3. A summarized product analysis for our CuO/ethane simulation at 2000 K.

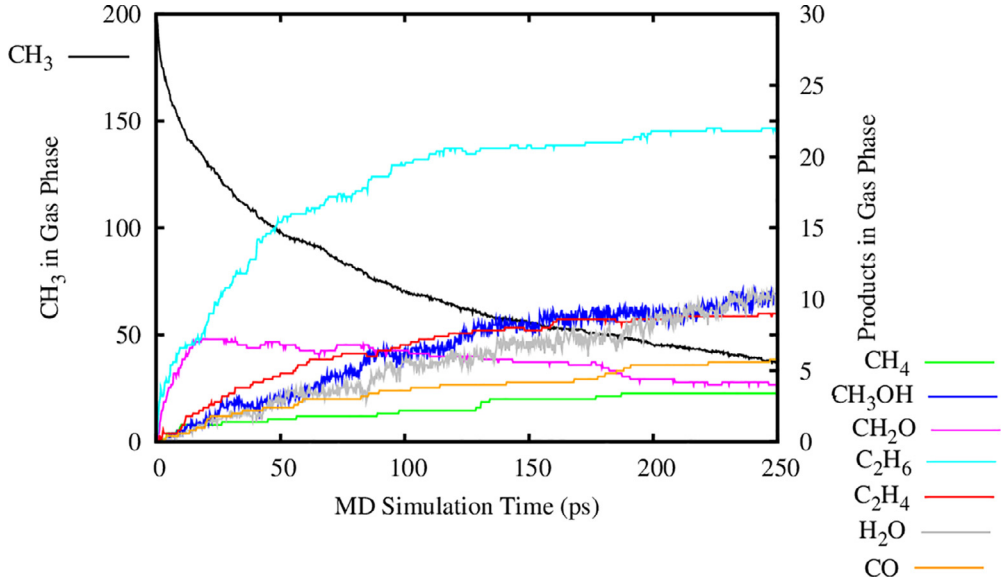

Fig. 4. A summarized product analysis for our CuO/ethylene simulation at 2000 K. A clear 2-stage kinetic for water formation was observed which reflects our previous analysis for fuel consumption.

radicals were utilized to skip the first H abstraction. An NVT ensemble was applied with Berendsen thermostat with a damping constant of 0.1 ps at 1000 K to match the experiment temperature.

4. Results and discussion

4.1. Simulation results

Before detailed product analysis, the hydrocarbon consumption was compared utilizing different fuels as shown in Fig. 2. With the simulation at 2000 K, the reactivity of ethane and ethylene were identical at around 0–50 ps. After 50 ps, ethylene molecules were more reactive than ethane. In addition, two reaction kinetics were identified for both fuels. For ethylene, the consumption rate at 0–100 ps is larger than at later time. It is possible that at early stage, fuel conversion was first dependent on surface reaction kinetics, while it shifts to oxygen-diffusion kinetics when surface active oxygen consumed. At later stages of simulation, a "fuel consumption limit" was observed. This limit

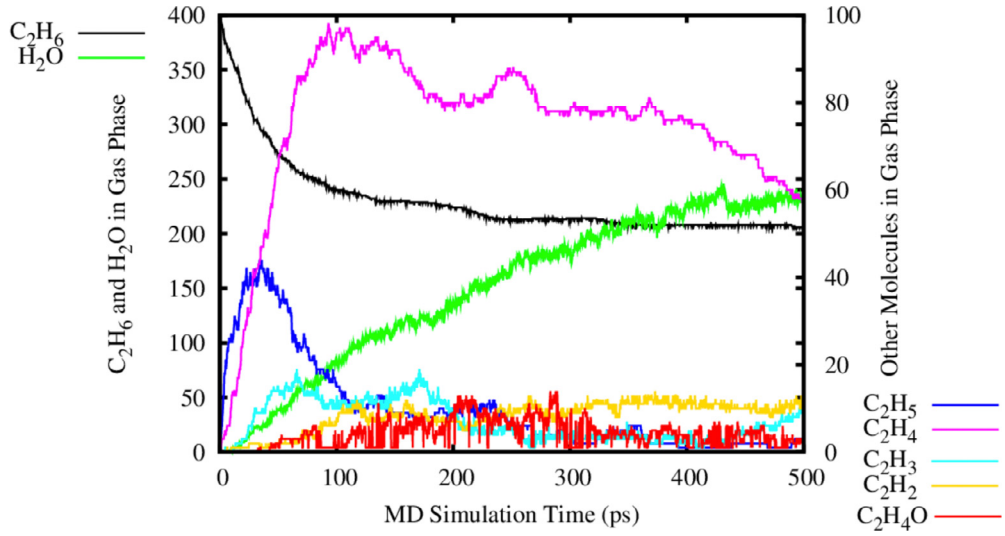

Fig. 5. A summarized product analysis for our CuO/methyl radical simulation at 1000 K

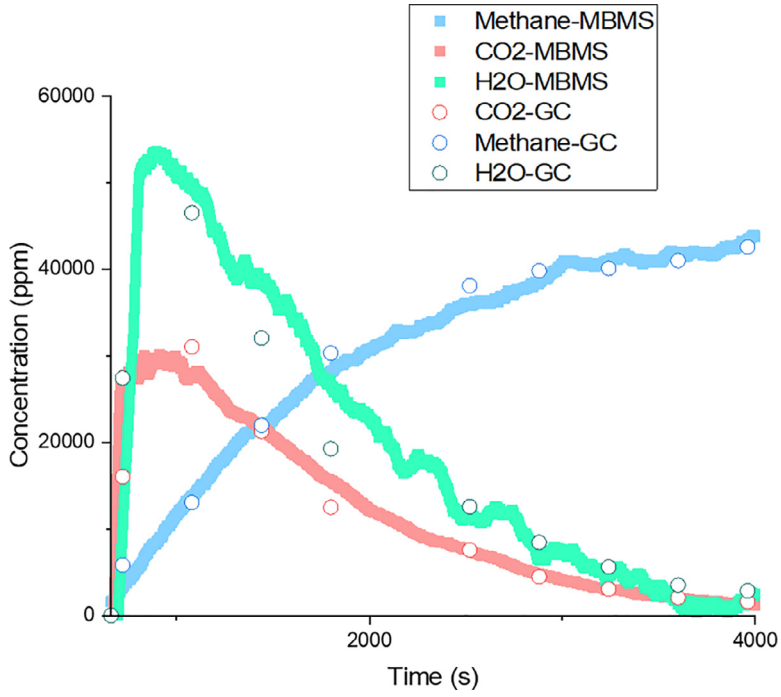

Fig. 6. Measured species from 5% Ethylene flown over 2 g pf CuO particles at 500 K.

indicates the time when the majority of reactive oxygen in the CuO particle was consumed. To prove this hypothesis, we extracted primary CuO particles when reaching this limit: that for ethane, a $Cu_{305}O_{86}$ primary particle was obtained at 250 ps while for ethylene a $Cu_{300}O_{39}$ particle was extracted at 450 ps.

Figure 3 shows the product analysis obtained from the simulation for ethane at 2000 K. Gas phase water molecules kept increasing even after ethane reached the consumption limits. This is because water comes from the combination of 2 hydroxyls (-OH) shown in Eq. (3). In this reaction, 1 oxygen from CuO moves to the gas phase. It has

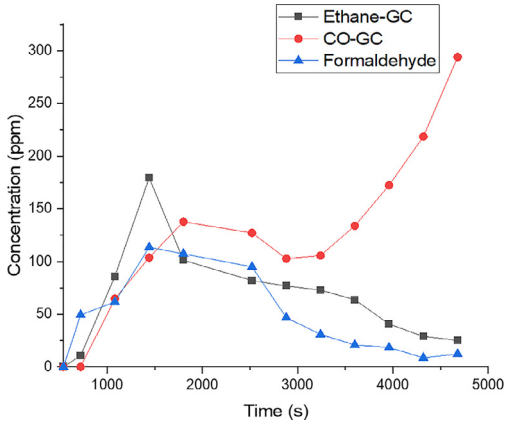

Fig. 7. Measured species from 5% Ethylene flown over 2 g of CuO particles at 800 K.

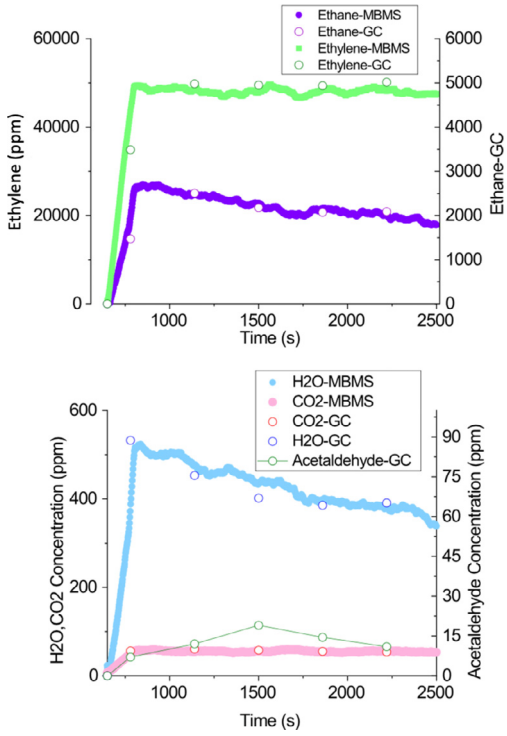

Fig. 8. MBMS and GC species detection for 5% Ethylene, 2 g of CuO particles, 200 scm total flow rate at: a) 500 K, b) 800 K.

been established that CuO thermal decomposition happens at 1000 K [11]. In the simulation, because of the small timescale applied (<1000 ps), there was no gas phase O_2 observed, thus the water formation indicates the reduction performance of fuels.

Sequential hydrogen abstractions were observed in the simulation where C_2H_5 radicals first exist in gas phase followed by C_2H_4, C_2H_3,

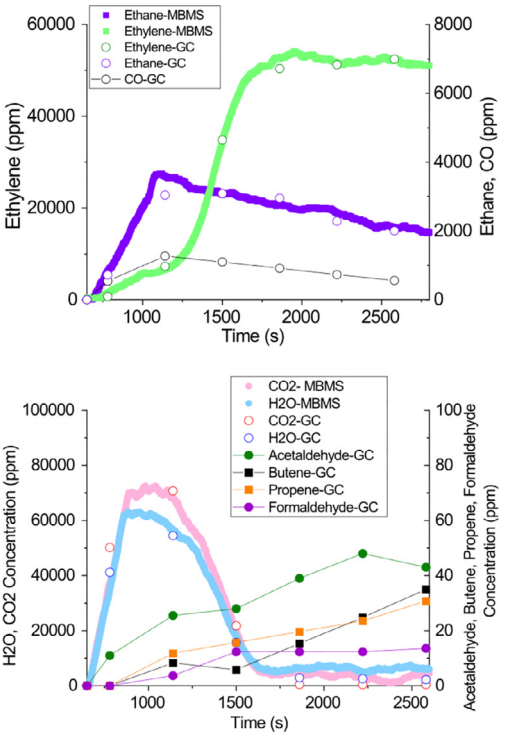

Fig. 9. MBMS and GC species detection for 5% Ethylene, 2 g of CuO particles, 200 scm total flow rate at: a) 500 K, b) 800 K.

and C_2H_2. This result can also explain the "fuel consumption limit" for ethane discussed previously. Because the ethylene is more reactive than ethane, the ethane-dominant environment shift to an ethylene-dominant environment, resulting in the ethane molecules not being consumed after 150 ps. In out simulation, C_2H_4O was observed in forms of formaldehyde (CH_3CHO) or combined with a single Cu atom (C_2H_4O–Cu) because of the high simulation temperature used. At the late stage of simulations, CO and large molecules like C_4H_8 were observed. Figure 4 shows the product analysis obtained from our simulation for ethylene at 2000 K. Like ethane analysis, a sequential abstraction trend was observed where C_2H_3 first exist in gas phase followed by C_2H_2. Comparing with ethane simulations, we observed water formation might follow a 2-stage kinetics in which the formation rate before 280 ps is faster than the rate after. This might be because at early stage, hydrogen abstraction was dominated by surface reaction, while it shifts to oxygen diffusion-dominant kinetics after the majority surface reactive oxygen is consumed. This water formation kinetics reflects our previous fuel consumption analysis, in which ethane consumption contains 2 reaction rates. In addition, products like 2 forms of C_2H_4O (CH_3CHO or C_2H_4O–Cu) and CO found in the ethane simula-

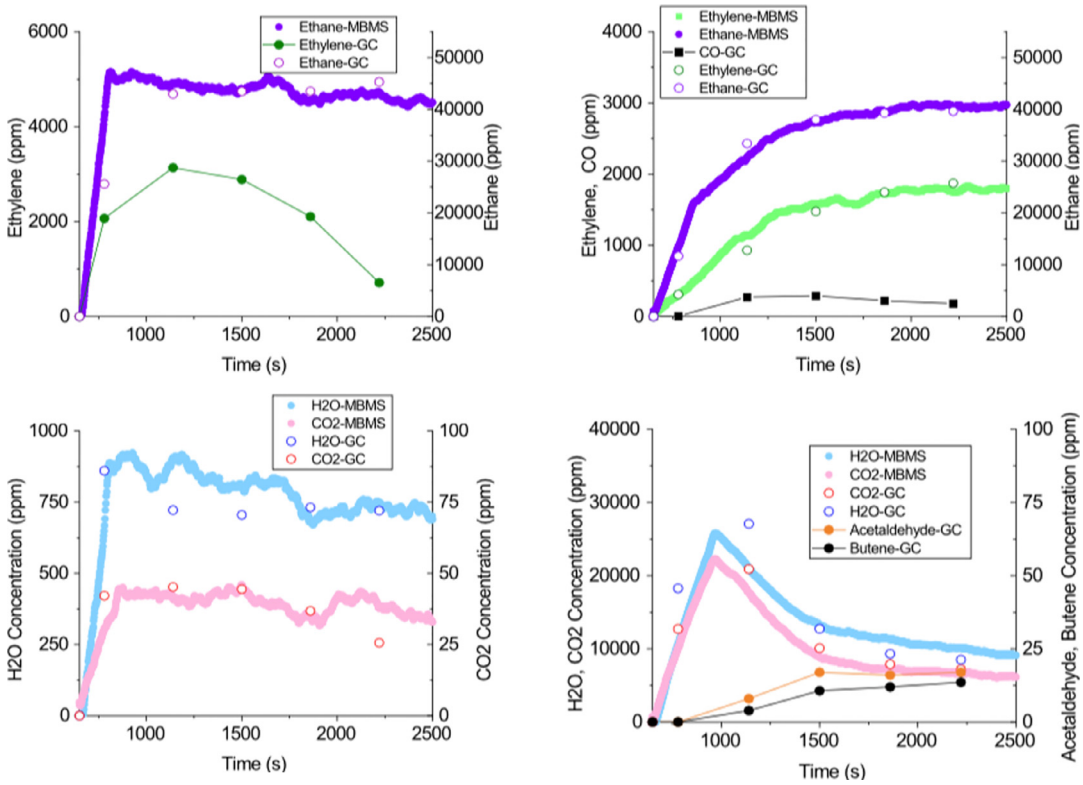

Fig. 10. Measured species from 5% Ethane flown over 2 g of CuO at: a) 500 K, b) 800 K.

tion were also observed in CuO/ethylene system. Figure 5 shows the product analysis obtained from Cu/methyl radical simulation at 1000 K.

This simulation might not fully reproduce the Cu/Methane chemistry because there are a number of ethane molecules observed in the gas phase from methyl combination. As the result, H_2O and C_2H_4 formation in this simulation was similar to what was obtained from C2 species analysis. On the other hand, utilizing methyl radical skips the first hydrogen abstraction, which allows us to obtain the late-stage methane chemistry at low temperature. We propose a formaldehyde formation mechanism in which methyl radical on CuO surface shown in Eq. (3):

$$CH_3 - O - Cu \rightarrow CH_2O + Cu - H \quad (3)$$

On CuO surface, those methyl radicals can go through further dehydrogenation to form CO shown in Eq. (4):

$$CH_3 - O - Cu \rightarrow Cu - 3H + CO \quad (4)$$

As shown in our product analysis, formaldehyde (CH_2O) was observed at early stage, which gas phase concentration reached maximum at 10 ps followed by CO formation in gas phase.

4.2. Experiment results

The concentration of major species for the oxidation of methane at 1000 K is shown in Fig. 6. Species were measured with both the MBMS and GC methods. There is a sharp initial spike in H_2O and CO_2 resulting from the complete oxidation of methane. As time progresses, the concentration of methane rises while the concentration of the complete combustion products of CO_2 and H_2O fall-off.

The addition species detected include ethane and carbon monoxide, which can be seen in Fig. 7. The concentration of CO is seen to rise as time progresses, which is understood to be a result of the decreasing amount of complete combustion when the oxygen on the particles becomes more consumed. Ethane, a result of CH_3 radical recombination, and formaldehyde, an incomplete oxidation species, were also detected with the GC. The results from the oxidation of ethylene at both 500 K and 800 K can be seen in Figs. 8 and 9. At 500 K, Fig. 8, it was found that ethylene was rather non-reactive, with the concentration of ethylene rising quickly, and the ppm concentrations of H_2O and CO_2 both being under 1000 ppm at all times. In addition to ethane, H_2O, and CO_2, both acetalde-

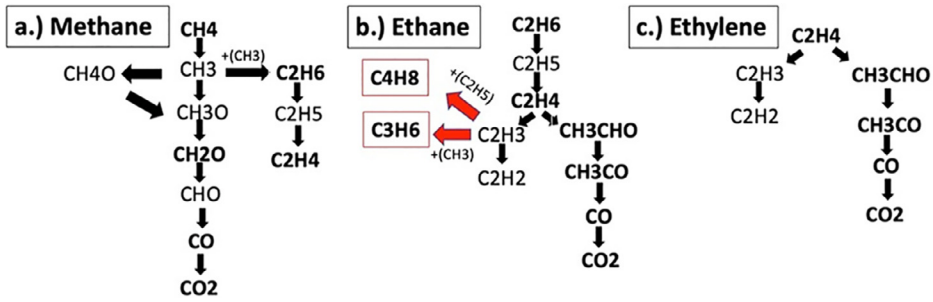

Fig. 11. Reaction pathway for the oxidation of methane, ethane, ethylene with CuO.

hyde and ethane were detected. At 800 K, Fig. 9, shows a variety of addition species were detected, including CO, butene, propene, and formaldehyde. Much more of the ethylene reacted, which can be seen by the lack of ethylene detected early in the experiment, and the corresponding large amounts of CO_2 and H_2O produced in Fig. 9. Acetaldehyde, butene, propene, and formaldehyde were found to generally increase with time, even as the quantities of CO_2 and H_2O fell. The concentration of CO peaked shortly before the amount of ethylene detected increased, with the CO rise indicating that the amount of complete combustion is decreasing and the consumption of ethylene would soon stop. Figure 10 similarly shows the detected species for the oxidation of Ethane at 500 K and 800 K. Like in the case of ethylene, ethane was found to be rather unreactive at 500 K with very little consumption of ethane. The only other species detected at this temperature were ethylene, a natural results from the first steps in the oxidation of ethane, and CO_2 and H_2O. No acetaldehyde was detected, unlike the case with ethylene. At 800 K, additional species of CO, acetaldehyde, and butene were detected. The consumption of ethane at 800 K in was found to be significantly less reactive than that of ethylene at the same temperature as seen in Fig. 7. This can be seen given how much less CO_2 and H_2O was measures with ethane as the fuel, and how more ethane was measured than earlier on during the experiment. The proposed reaction networks for methane, ethane, and ethylene resulting from the experimental and simulation results is shown in Fig. 11.

5. Conclusion

Reaction pathways for the oxidation methane, ethane, and ethylene with CuO was obtained by ReaxFF simulations between temperatures of 1000 K and 2000 K. Experiments in a fixed-bed flow reactor were preformed with methane, ethane, and ethylene at temperatures ranging from 500 K to 1000 K with species measurements from an EI-MBMS and GC. The simulation and experiment agree on the production of such species as CH_3CHO, CH_2O, CO, and H_2O, which allowed for the creation of C1 and C2 reaction pathways which can be used in kinetic models of C2 species and larger. The simulation and experiment disagree on the formation of C_2H_2, CH_3 OH, and CO_2, with large amounts of C_2H_2 being measured in the ethylene oxidation simulations and CH_3OH being formed in methane oxidation simulations, while neither species was experimentally found. In the case of CO_2, little-to-no CO_2 was seen in simulations. This results from the short simulation timescale, preventing full oxidation. The differences between simulation and experiments in products produced allow for the potential to modify the ReaxFF force field to more accurately model Cu–H–O–C reaction kinetics.

Declaration of Competing Interest

None.

Acknowledgments

This work was funded under DOE – NETL Project Number: DE-FE0026825; Sub-award number 0004-PSU-DOE-6825.

Supplementary material

Supplementary material associated with this article can be found, in the online version, at doi:10.1016/j.proci.2020.06.006.

References

[1] J. Adanez, A. Abad, F. Garcia-Labiano, P. Gayan, L.F. de Diego, *Progr. Energy Combust. Sci.* 38 (2012) 215–282.
[2] A. Olafsen, C. Daniel, Y. Schuurman, L. Råraberg, U. Olsbye, C. Mirodatos, *Catal. Today* 115 (2006) 179–185. Proceedings of the 8th International Conference on Carbon Dioxide Utilization.

[3] E.R. Monazam, R. Siriwardane, R.W. Breault, H. Tian, L.J. Shadle, G. Richards, S. Carpenter, *Energy Fuels* 26 (2012) 2779–2785.
[4] E. A. Goldstein, R. E. Mitchell, *Proc. Combust. Inst.* 33 (2011) 2803–2810.
[5] H. Zhao, X. Yang, Y. Ju, *Combust. Flame* 173 (2016) 187–194.
[6] H. Zhao, J. Fu, F.M. Haas, Y. Ju, *Combust. Flame* 183 (2017) 253–260.
[7] A.C.T. van Duin, S. Dasgupta, F. Lorant, W.A. Goddard, *J. Phys. Chem. A* 105 (2001) 9396–9409.
[8] A.C.T. van Duin, Reaxff User Manual 2002, 1–39, https://www.engr.psu.edu/ADRI/Upload/reax_um.pdf.
[9] S. L. Mayo, B. D. Olafson, W. A. Goddard, *J. Phys. Chem.* 94 (1990) 8897–8909.
[10] A.K. Rappe, C.J. Casewit, K.S. Colwell, W.A. Goddard, W.M. Skiff, *J. Am. Chem. Soc.* 114 (1992) 10024–10035.
[11] N.L. Allinger, Y.H. Yuh, J.H. Lii, *J. Am. Chem. Soc.* 111 (1989) 8551–8566.
[12] W. Hu, F. Donat, S.A. Scott, J.S. Dennis, *RSC Adv.* 6 (2016) 113016–113024.
[13] T.P. Senftle, et al., *Nat. Comput. Mater.* 2 (1) (2016) 15011.